DEUTSCHES ELEKTRONEN-SYNCHROTRON DESY

DESY 88-121
August 1988

B-MESON FACTORIES

by

H. Kolanoski
Institut f. Physik, Universität Dortmund

ISSN 0418-9833

NOTKESTRASSE 85 · 2 HAMBURG 52

To be sure that your preprints are promptly included in the
HIGH ENERGY PHYSICS INDEX ,
send them to the following address (if possible by air mail) :

DESY
Bibliothek
Notkestrasse 85
2 Hamburg 52
Germany

DESY 88-121
August 1988

ISSN 0418-9833

B-Meson Factories*

H. Kolanoski
Institut für Physik, Universität Dortmund, Fed. Rep. of Germany

Abstract

This lecture surveys current ideas and proposals for high-luminosity e^+e^- machines which could be available in the 90ties as B-meson factories. Different solutions are compared: upgrades of existing machines, new storage rings, linear colliders and asymmetric machines. Concepts for B-factory detectors are discussed emphasizing their particle identification and vertex detection capabilities.

1 Introduction and Overview

1.1 Basic Motivation for B-Factories

One of the fundamental questions in particle physics is: Why do fermions occur in families? Related to this 'generation puzzle' are the questions:

- How many families exist?
- What is the origin of the masses of fermions?
- What is the systematics in the transitions between families?
- What is the source of CP-violation?

There is a good chance that extensive studies of the properties of the third family, the leptons τ and ν_τ and the quarks b and t (the latter as yet undiscovered), could provide us with clues for these questions. Progress is expected from high statistics measurement of rare decay modes. In particular, after the discovery of B^0-$\overline{B^0}$ mixing by the ARGUS group [1], there is a realistic chance to observe CP-violation in the $B - \overline{B}$ system. Establishing CP-violation in another than the kaon system is certainly one of the most important future experiments. But it is also most demanding with respect to the required luminosity. In the most optimistic case at least 10^7 $B\overline{B}$ events are required for the observation of CP-violation, more probably something like 10^9 $B\overline{B}$ events are needed. This has to be compared to the several 10^5 $B\overline{B}$ now available from $\Upsilon(4s)$ decays. With 10^7 to 10^9 $B\overline{B}$ events, which eventually could be provided by dedicated B-factories, the study of a large variety of rare B and τ decays becomes possible opening windows to potentially new physics.

*Lecture given at the XVI International Meeting on Fundamental Physics 'CP Non-Conservation and B Physics', Peñiscola (Castellón), Spain, April 25-29, 1988.

Machine	$\sqrt{s_{max}}$ [GeV]	$L_{peak}(\Upsilon(4s))$ [$cm^{-2}s^{-1}$]	σ_E ($\Upsilon(4s)$) [MeV]
CESR	16	$8 \cdot 10^{31}$	4.0
DORIS-II	11	$2 \cdot 10^{31}$	10.5
VEPP-4	14	$3 \cdot 10^{30}$	8.0

Table 1: e^+e^- machines presently running in the Υ energy region. From [2].

1.2 Present Status of b-Physics Experiments

Most of the experimental information on the third fermion family stems from experiments at the e^+e^- colliders CESR (Cornell), DORIS-II (Hamburg) and VEPP-4 (Novosibirsk) running in the region of the $b\bar{b}$ threshold (see Table 1). The continuum machines PETRA and PEP contributed b-lifetime measurements from b-jets. The detectors CLEO and ARGUS are most suited to reconstruct B-meson decays. Until recently the CLEO group had accumulated at the $\Upsilon(4s)$ resonance an integrated luminosity of about 350 pb^{-1} yielding about $7 \cdot 10^5$ produced $B\overline{B}$ pairs. The corresponding numbers for ARGUS are about 100 pb^{-1} and about $2 \cdot 10^5$ $B\overline{B}$ pairs. It is clear that these experiment are sensitive only to decays with branching ratios larger than about 10^{-4}, which may be extended to about 10^{-5}. Further improvements can only be achieved by new machines with much higher luminosities. The goal of these B-meson factories is to reach at least 10000 pb^{-1} per year.

1.3 Detector Requirements

With current detectors the reconstruction efficiencies for B-meson decays at the $\Upsilon(4s)$ is only about 10^{-3}. $B\overline{B}$ events have typical average charged multiplicities of 8, with about the same number of photons. Since at the $\Upsilon(4s)$ the B's are produced nearly at rest ($p_{lab}(B) \approx$ 300 MeV) the decay products of the B and the $\overline{B}$ are completely intermixed yielding large combinatorial background in the reconstruction procedure. This background is even more increased by the limitations in the particle identification (typically π/K separation below about 0.700 to 0.900 GeV, K/p separation below 1.2 to 1.5 GeV with dE/dx and time-of-flight measurements).

In the continuum the b and $\bar{b}$ jets are at suffiently large energy well separated. However, this advantage is more than cancelled by the large number of additional fragmentation products and even more limited particle identification possibilities.

Thus it became clear that the increase of luminosity has to go along with an improvement of the detectors. The performance of new detectors is commonly gauged with the upgraded CLEO detector [3]. Further improvements are expected in two points:

- particle identification up to the heighest momenta occurring in B-decays (2.5 GeV/c);
- vertex detection with an accuracy in the order of 10 μm to tag D's or even B's by their secondary vertex.

Machine	energy	L [$cm^{-2}s^{-1}$]	L/day	$\sigma_{b\bar{b}}$	$\frac{\sigma_{b\bar{b}}}{\sigma_{had}}$	$N_{b\bar{b}}$/year
CESR	$\Upsilon(4s)$ (thresh.)	$2 \cdot 10^{32}$	15 pb^{-1}	1	0.25	$2.0 \cdot 10^6$
BMF	$\Upsilon(4s)$ (thresh.)	$> 10^{33}$	86 pb^{-1}	1	0.25	$1.0 \cdot 10^7$
PEP	25 GeV (cont.)	$6 \cdot 10^{31}$	5 pb^{-1}	0.046	0.09	$2.7 \cdot 10^4$
SLC	Z^0	$5 \cdot 10^{29}$	43 nb^{-1}	6.6	0.20	$3.3 \cdot 10^4$
LEP	Z^0	$1 \cdot 10^{31}$	860 nb^{-1}	6.6	0.20	$6.6 \cdot 10^5$

Table 2: e^+e^- machines available in the early nineties for b- physics. From [4].

Machine	type	$\sqrt{s_{max}}$ [GeV]	$\frac{\sigma_{b\bar{b}}}{\sigma_{tot}}$	$N_{b\bar{b}}$/year
TEV II	p (fixed target)	45	10^{-6}	10^8
UNK	p (fixed target)	75	10^{-5}	10^7
TEV I	$p\bar{p}$	2000	10^{-4}	10^8
HERA	ep	314	10^{-3}	10^5
SSC	pp	40000	10^{-4}	10^{11}

Table 3: Potential for b-physics at hadronic machines.

1.4 B-Physics in the Near Future

Table 2 contains a list of e^+e^- machines which will probably be available for b-physics through the nineties. Besides the threshold machines CESR (with luminosity upgrade, see Sect.2.2.4) and a yet to be built B-meson factory (BMF), the table containes also the PEP and LEP storage rings and the linear collider SLC where b-$\bar{b}$ jets can be studied in the continuum or on the Z^0 resonance. Figure 1 shows that the Z^0 is a nice b,c and τ factory with a $b\bar{b}$ cross section about 5 times larger than at the $\Upsilon(4s)$. However, the above mentioned difficulties for the reconstruction of B's within jets apply also in this case. Large $b\bar{b}$ rates are also expected at hadron colliders (see Table 3). In particular, the rate at the SSC would be enormous. However, with presently conceivable experimental techniques only a small fraction of these rates would be detectable. Studies for the different machines can be found in [4,5,6,7].

1.5 B-Meson Factory Projects (or Ideas)

In many laboratories experimental, theoretical and machine physicists startet thinking about a B-meson factory (Table 4). These projets are in very different stages of preparation. The upgrade program of CESR is successfully progressing since some time, other projects are in the proposal phase like the PSI project (PSI = Paul-Scherrer-Institut, formerly SIN) and others are more in an exploratory phase like the 'asymmetric machines' discussed at DESY

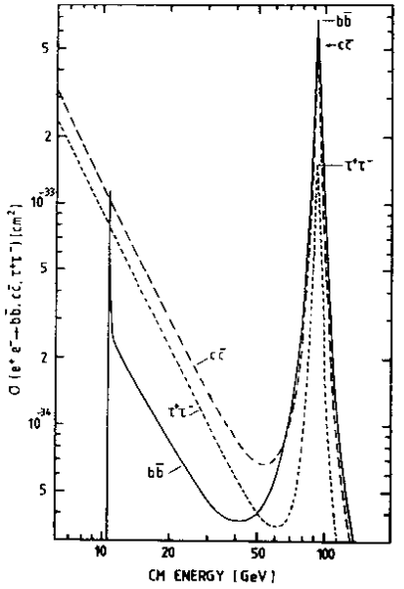

Figure 1: Cross section for the e^+e^- production of $c\bar{c}$, $\tau^+\tau^-$ and $b\bar{b}$ pairs. From [8].

and SLAC.

1.6 Physics Goals of a B-Meson Factory

For the discussion of the physics goals of a B-meson factory let us concentrate on e^+e^- machines running on the $\Upsilon(4s)$. At higher energies, e.g. at the $\Upsilon(5s)$, also B_s and may be even B_c production could be investigated. Assuming that a luminosity of L = 10^{33} $cm^{-2}s^{-1}$ can be reached the integrated luminosity will be about 10000 pb^{-1} per year (with an overall efficiency of 30%). This gives following event yields per year:

- $1 \cdot 10^7$ $B\overline{B}$,
- $2 \cdot 10^6$ $\tau^+\tau^-$,
- $7 \cdot 10^6$ $c\bar{c}$,
- $2 \cdot 10^7$ $u\bar{u}$, $d\bar{d}$, $s\bar{s}$.

Though the main physics goal is clearly the study of B-decays the high luminosity will allow for significant contributions also to other fields. A physics program will include the following points:

- B-decays:
  - weak currents, CMK matrix (b→u);

laboratory	project	status	reference
Cornell	upgrade CESR	continuing	[9]
KEK	upgrade AR (accumulator ring)	proposal	[10]
PSI/SIN	double ring	proposal	[11,12]
Frascati	linear collider (s.c.)	proposal	[13]
UCLA	linear collider (n.c.)	study	[14]
SLAC	PEP upgrade asym.machine (PEP)	completed study	[15] [16]
DESY	asym.machine (PETRA)	study	[17]
Novosibirsk	double ring	study	[18]

Table 4: B-factory projects (e^+e^- machines).

  - strong interaction influence;
  - rare B decays (penguins, ...);
  - mixing (B_d, B_s);
  - CP-violation.

- τ-decays:
  - spectral functions;
  - spin correlations;
  - meson spectroscopy;
  - lepton flavour violation;
  - mass of ν_τ.
- heavy-quark spectroscopy:
  - Υ family;
  - B_u, B_d, B_s, B_c...;
  - charmed mesons and baryons;
- QCD-topics:
  - α_s from $\Upsilon \to \gamma gg$;
  - fragmentation;
  - total hadronic cross section.

- Two-photon physics:
  - light quark spectroscopy (up to charm);
  - glueballs, four-quark states;
  - two-photon total cross section.

2 B-Factory Machines

2.1 Machine Concepts for B-Factories

Different machine concepts are currently considered for high luminosity B-factories. We will discuss in the following the alternatives:

- storage ring versus linear collider,
- threshold machine versus continuum machine
- symmetric machine versus asymmetric machine (boosted e^+e^- system)

Storage ring machines: The clear advantage of a storage ring concept is the well known technology. Long standing experience can be used to obtain optimal luminosities, estimated to be larger than 10^{33} $cm^{-2}s^{-1}$.

Storage ring projects are the upgrades of CESR and the Tristan accumulator ring (AR), and the B-factory project at PSI/SIN and at Novosibirsk (see Table 4).

Linear colliders: Linear colliders with the required high luminosities certainly need a lot of development work. R & D in this field is very challenging and rewarding in view of future accelerator concepts. The suggested luminosities of 10^{34} $cm^{-2}s^{-1}$ are about five orders of magnitude larger than the design luminosity of SLC which is still far from being reached [19,20]. Linear collider projects are pursuit at UCLA with normal conducting cavities and in Frascati with superconducting cavities (seeTable 4).

Threshold machines: These are machines which could run in the energy region closely above the threshold for open bottom production, especially at the $\Upsilon(4s)$ and $\Upsilon(5s)$ resonances. The advantage of B-Meson production on these resonances is the large cross section ($\sim$ 1 nb) at the $\Upsilon(4s)$, the well defined quantum numbers of the initial state ($J^{PC} = 1^-$) and the exclusive production of $B\overline{B}$ pairs (at least on the $\Upsilon(4s)$). The last point allows for tagging a B ($\overline{B}$) by reconstructing the $\overline{B}$ (B). Unfortunately the reconstruction of B-mesons at threshold is difficult: the B's are produced nearly at rest so that the decay products are not separated. This leads to a large combinatorial background for reconstructed B's. For the same reason the B-meson lifetimes cannot be measured (decay length at the $\Upsilon(4s)$: 20 μm) and the decay products of the B and $\overline{B}$ cannot be separated by their decay vertices.

Continuum machines: At higher energies the decay products of the hadrons containing the b and $\bar{b}$ quarks are boosted into opposite hemispheres and their decay vertices are better separated (more than about 400 μm for $\beta\gamma > 1$). The prize one has to pay for this advantage over threshold machines is a large number of additional fragmentation products. Also the particle identification becomes at high energies more difficult (except for leptons).

A good compromise between b-$\bar{b}$ separation and decreasing cross section can be found around 20 GeV cms energy where the upgraded PEP machine with the TPC/$\gamma\gamma$ experiment as the only detector will run in the future [15]. A large $b\bar{b}$ cross section is provided by the Z^0 decays to be observed at SLC and LEP (see Fig.1 and Table 4).

Asymmetric machines: It has been suggested [21] that the advantages of threshold and continuum machines could be combined in machines with different electron and positron energies. The energies can be chosen so that the $\Upsilon(4s)$ or $\Upsilon(5s)$ resonances are produced with a boost along the beam direction. The boosted B-mesons then have correspondingly larger decay lengths (for $\beta\gamma = 1$ a decay length of about 400 μm is obtained).

This concept has been discussed at SLAC [16] and DESY [17]. A suitable optical system which is able to focus both the high energy (12 GeV) and low energy (2 GeV) beams and keeping at the same time the synchrotron radiation out of the detector is still under investigation. Also a detector has to be developped which can exploit the advantage of longer decay lengths.

2.2 Storage Rings as B-Factories

Before we discuss the different projects for high luminosity storage rings we first discuss some of the major effects limiting the luminosity.

2.2.1 The luminosity formula

The luminosity L of interacting particle beams is the proportionality factor connecting a reaction cross section σ with the observed rate $\dot{N}$ of this reaction:

$$\dot{N} = L\sigma \tag{1}$$

If we consider the e^+ beam bunch hitting the e^- bunch the relative number of reactions is

$$\frac{dN}{N_+} = \frac{N_-\sigma}{A} \tag{2}$$

Here N_+, N_- are the number of particles in the e^+ and e^- bunch, respectively. If the bunches cross with a frequency $f = n_b \cdot f_0$, where n_b is the number of bunches in a beam and f_0 the circulation frequency of the ring, we obtain by combing (1) and (2):

$$L = \frac{N_+N_-f}{4\pi\sigma_x\sigma_y} = \frac{I_+I_-n_b}{4\pi e^2 f_0\sigma_x\sigma_y} \tag{3}$$

This is the basic luminosity formula, which essentially tells us that the beam currents have to be large and the beam cross sections at the intersection points have to be small. We will see in the following that these are rather conflicting requirements.

2.2.2 Some machine physics

In a periodic machine (without damping) the horizontal (x) and vertical (y) deviations of a particle trajectory from the reference orbit are given by:

$$x(s) = a_x\sqrt{\beta_x(s)}\cos(\phi_x(s) - \delta_x)$$
$$y(s) = a_y\sqrt{\beta_y(s)}\cos(\phi_y(s) - \delta_y)$$

s is the coordinate along the reference orbit (see Fig. 2). The initial conditions at $s = s_0$ determine the amplitudes a_x, a_y and the phases δ_x, δ_y.

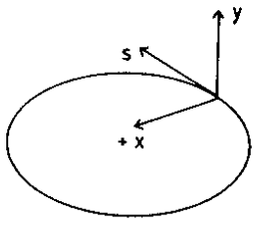

Figure 2: Coordinate system along the reference orbit.

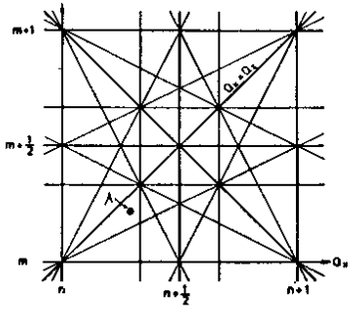

Figure 3: Stability diagram for the horizontal and vertical betatron tune.

The horizontal and vertical betatron functions $\beta_x(s)$, $\beta_y(s)$ **can be calculated from** the magnet lattice. They describe the variations of both the amplitude and the phase of a trajectory as it develops in s:

$$\begin{aligned} \textit{amplitude}: &\quad \sim \sqrt{\beta(s)} \\ \textit{phase}: &\quad \phi(s) = \int_{s_0}^{s} \frac{dt}{d\beta(t)} \end{aligned}$$

Since the betatron functions are periodic (L= ring circumference),i.e.

$$\beta(s) = \beta(s+L),$$

the number of betatron oscillations per turn is constant both for the horizontal and vertical movements:

$$Q_{x,y} = \frac{1}{2\pi} \oint \frac{ds}{\beta_{x,y}(s)}$$

A stable working point of the machine has to fulfill the condition:

$$mQ_x + nQ_y \neq l \tag{4}$$

where m,n,l are not too large integer numbers. Dangerous resonances, which should be as far as possible from the working point, are drawn as lines in the stability diagram in Fig.3. The stability condition (4) implies in particular that a given trajectory never arrives with the same phase at the same place in the machine. At fixed s=s_1 a trajectory (defined by the initial conditions a and δ) describes an ellipse in the phase space (x, x') or (y, y') as shown in Fig.4. The representation of the ellipses is (z=x,y):

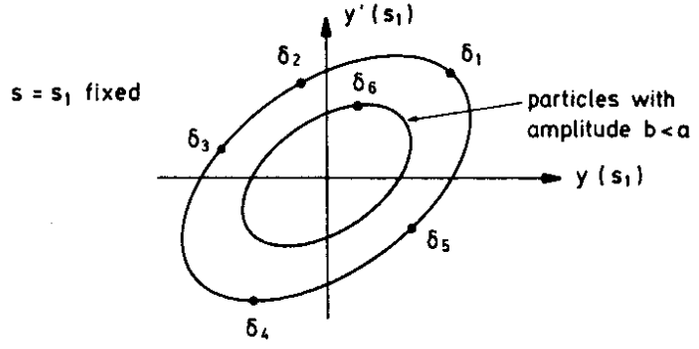

Figure 4: Phase ellipse of a trajectory at a fixed s=s_1.

$$\begin{aligned} z &= a_z\sqrt{\beta_z}\cos(\phi_z - \delta_z) \\ z' &= -\frac{a}{\sqrt{\beta}}\left[\sin(\phi_z - \delta_z) - \beta_z' \cos(\phi_z - \delta_z)\right] \end{aligned}$$

The shape of the phase ellipse changes as one goes from s=s_1 to another point s, but the area of the ellipse is a constant of motion:

$$Area = \pi \cdot a_z^2.$$

The amplitudes of a given trajectory at a fixed point s are always smaller than $a_z\sqrt{\beta_z(s)}$. The trajectory with the maximal amplitude defines the beam enveloppe (Fig.5):

$$z_{max}(s) = \sqrt{\epsilon_z \beta_z(s)} \quad (z = x, y).$$

Here we have introduced the emittance $\epsilon_z = a_{zmax}^2$. In the usual case of gaussian shaped beams the emittance defines the 1-σ spread of the beams:

$$\sigma_{x,y}(s) = \sqrt{\epsilon_{x,y}\beta_{x,y}(s)} \tag{5}$$

If both beams are gaussian with the same spread, the effective collision area is:

$$A(s) = 4\pi\,\sigma_x\sigma_y. \tag{6}$$

Up to now radiation processes have not been included. In e^+e^- machines the horizontal oscillations are damped by the radiation and at the same time excited by the quantum fluctuations. The equilibrium between both effects determines the natural horizontal emittance, ϵ_{x0} with an energy dependence

$$\epsilon_{x0} = E^2\hat{\epsilon}_{x0},$$

with $\hat{\epsilon}_{x0}$ defined as the emittance at 1 GeV. The vertical emittance is induced by a horizontal-vertical coupling described by the parameter k which is typically a few percent. With this coupling the emittances are:

$$\epsilon_x = \frac{\epsilon_{x0}}{1+k}; \quad \epsilon_y = \frac{k\cdot\epsilon_{x0}}{1+k}.$$

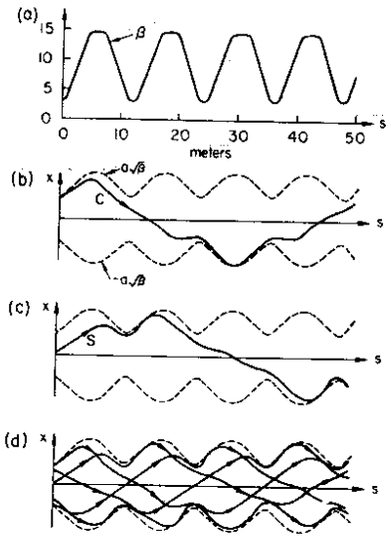

Figure 5: (a) **Betatron function.** (b) **and (c) Cosine- and Sine- like trajectories.** (d) One trajectory on several successive revolutions. The dashed line is the enveloppe. From [23].

This gives for the area of the beam according to (5,6):

$$A(s) \;=\; 4\pi\, E^2 \hat{\epsilon}_x \sqrt{k\beta_x\beta_y}.$$

At the interaction point A(s) should be small which could be achieved by making ϵ_x, k, β_x or β_y small. However, as one might have expected all these quantities cannot be made arbitrarily small.

Beam-beam tune shift: The most serious limitation comes from the beam-beam interaction at the intersection points: the bunches focus each other leading to 'tune-shifts' ΔQ_x and ΔQ_y which, as it turns out cannot be fully compensated.

An additional focussing element with the quadrupole strength Δk changes the Q-value (either in x or y):

$$\Delta Q \;=\; \frac{1}{4\pi}\int \beta(s)\Delta k(s)ds\,.$$

Thus the effect is large if the betatron function is large in the region of the additional quadrupole field. Since the quadrupole stength is momentum dependent, k = eg/p, the tune shift is as well. The change of the tune with the momentum, the chromaticity ξ, is given by an integral over all quadrupoles in the machine:

$$\xi \;=\; \frac{\Delta Q}{\Delta p/p} \;=\; -\frac{1}{4\pi}\int_{quads} \beta(s)k(s)ds\,. \qquad (7)$$

Thus a given momentum spread of the machine yields a tune spread which, however has to be confined within resonance lines in the Q_x-Q_y diagram (Fig.3). Equation (7) suggests to make the betatron function not too large in the quadrupoles.

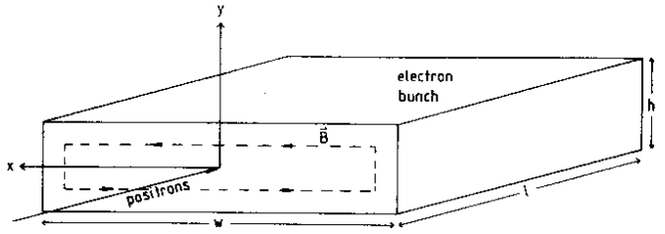

Figure 6: **Rectangular bunch model to explain the space charge effect for colliding** bunches.

Let us now turn to the tune shift caused by the beam-beam interaction. Assuming a restangular bunch cross section as in Fig.6 the field seen by a e^+ is obtained from:

$$I \;=\; \frac{1}{\mu_0}\int Bds \;\approx\; \frac{2wB}{\mu_0}\,(for\ \sigma_x \gg \sigma_y).$$

The positron passes through the charge $Q \;=\; N\cdot e\cdot 2y/h$ in the time $t \;=\; l/2c$ yielding the current

$$I \;=\; \frac{Ne\,2y\,2c}{hl}.$$

The corresponding B-field increases in this approximation ($\sigma_x \gg \sigma_y$ and rectangular profile) in vertical direction linearly with y like a quadrupole field

$$B \;\approx\; B_x(y) \;=\; \frac{2\mu_0 Nec}{whl}y \;=\; g\cdot y\,.$$

With the beam-beam induced quadrupole strength $k_{b-b} = eg/p_0$ the vertical tune shift becomes

$$\Delta Q_y \;=\; \frac{1}{4\pi}\int_0^l k_{b-b}\beta_y(s)ds \;\approx\; k_{b-b}\,\beta_y^* l$$

(β_y^* is the β-function at the intersection point). In practice the assumption of a rectangular beam profile is very bad. For a gaussian profile the field is linear only in the center, the gradient even reverses its sign at the periphery. The horizontal and vertical tune shifts are then given by:

$$\Delta Q_{x,y} \;=\; \frac{r_e\beta_{x,y}^* N}{2\pi\gamma\sigma_{x,y}^*(\sigma_x^* + \sigma_y^*)}$$

(r_e = classical electron radius, γ = Lorentz factor, the '*' is assigned to values at the interaction point). This tune shift is for gaussian beam profiles actually a tune spread in the Q_x-Q_y diagram which cannot be compensated by additional quadrupoles. Emperically, ΔQ cannot exceed some maximum value ($\Delta Q_{max} \approx 0.025$ to 0.05) which, for a given beam optics, limits the number of electrons N per bunch.

Optimum luminosity is reached if the horizontal and vertical tune shifts are equal ($\Delta Q = \Delta Q_x = \Delta Q_y$) which yields the condition:

$$\frac{\beta_y^*}{\beta_x^*} \;=\; \frac{\epsilon_y}{\epsilon_x}.$$

The tune shift becomes in this case:

$$\Delta Q \;=\; \frac{r_e N}{2\pi\gamma\epsilon_{x0}},$$

which, substituted into the luminosity formula (3), yields:

$$L = \frac{\pi}{e^2 r_e^2} \frac{n_b f_0 E^4 (1+k) \hat{\epsilon}_{x0}}{\beta_y^*} \Delta Q^2 \qquad (8)$$

$$(\pi/(e^2 r_e^2) = 1.513 \cdot 10^{32}\, cm^{-2} s^{-1} GeV^{-4}).$$

The luminosity can now be optimized by tuning the parameters:

- The bunch crossing frequency $n_b \cdot f_0$ should be large (i.e. for a given ring: n_b large).
- The horizontal emittance should be large.
- The tune shift should reach the maximal value.
- The vertical β function at the intersection point should be as small as possible.

Limitations on β_y^*: Around a symmetry point in a free drift space, as it is the case in the interaction region, the β-function quadratically increases with the distance from the symmetry point:

$$\beta_y(s) = \beta_y^* + \frac{s^2}{\beta_y^*}.$$

This means $\beta_y(s)$ becomes large for small β_y^*, which is a consequence of Liouville's theorem (the divergence is largest in a focus). The above formula poses two constraints on β_y^*:

- In the interaction region β_y should not vary by more than about a factor 1.5 over the bunch length σ_l:

$$\frac{\beta_y(s)}{\beta_y^*} = 1 + \left(\frac{\sigma_l}{\beta_y^*}\right)^2 \leq 1.5 \Rightarrow \beta_y^* \geq 1.5\sigma_l. \qquad (9)$$

- A large $\beta_y(s)$ in the quadrupoles contributes to the chromaticity, which eventually limits the aperture of the machine (dynamical aperture). For small β_y^* the β-function in the quadrupoles can only be kept reasonably small by moving as close as possible to the intersection point (mini-β or micro-β schemes).

2.2.3 The PSI/SIN B-Factory Project

A B-meson factory project at the Paul-Scherrer Institut in Switzerland (PSI, formerly SIN) is under discussion since about two years [11]. A proposal (for the machine and detectors), worked out by a Swiss-German-French group, will soon be submitted to the Swiss authorities [12].

The luminosity goal

$$L > 10^{33}\, cm^{-2} s^{-1}$$

at the $\Upsilon(4s)$ should be reached in an e^+e^- storage ring following the basic construction principles [12]:

- double ring (Fig.7) with

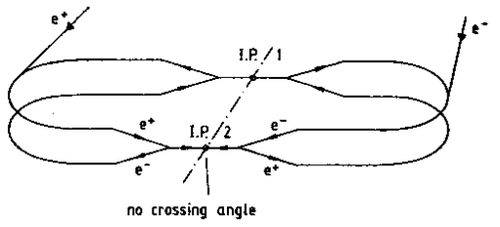

Figure 7: Principle design of the PSI/SIN B-factory.

- many bunches which collide
- head-on focussed by a
- mini(μ)-β scheme.

The ring will operate at beam energies between 1 and 7 GeV providing luminosity in two interaction regions. The high luminosity will be achieved by optimizing the parameters in the luminosity formula (8) in the following way:

- A large number of bunches n_b:

  In a single ring one has $2n_b$ crossing points, which all contribute to a beam disturbance. A separation of the beams outside the interaction regions is most directly achieved in a double ring machine. The luminosity limitations in the original double ring machine DORIS are understood to be due to the finite crossing angle causing instabilities by longitudinal-transverse couplings of the bunch oscillations [24]. Therefore a suitable beam separation scheme has to allow for head-on collisions.

  With an accelerating RF of 500 MHz and the ring circumference of 648 m the harmonic number is $1080 = 2^3 \cdot 3^3 \cdot 5$ allowing for n_b = 1,2,3,4,5,6,8,9,10,12,15,18, 20,24.... Given a 32 m space between the beam separators near the IR the maximum bunch number will be about 20.

- A large horizontal emittance ϵ_{x0}:

  The horizontal aperture of the ring is limited to $A_{max} \approx 50\, mm$ by the vacuum chamber and nonlinear fields. Requiring that the aperture contains $N \cdot \sigma$ of the beam where N is between 7 and 10, one obtains a relation for the maximal allowable emittance:

$$A_{max} = N\sigma_{max} = N\sqrt{\epsilon \cdot \beta_{max}} \Rightarrow \epsilon_{max} = \frac{A_{max}^2}{N^2 \beta_{max}}.$$

  Because of this relation the β-function is kept below 30 m in the whole ring.

- A small vertical β-function β_y^* at the interaction regions:

  The limitation comes according to (9) from the bunch length ($\sigma_l \approx 2\, cm$ for 500 MHz): $\beta_y^* \geq 3\, cm$. This will be achieved with mini-β quadrupoles placed about 70 cm from the interaction region.

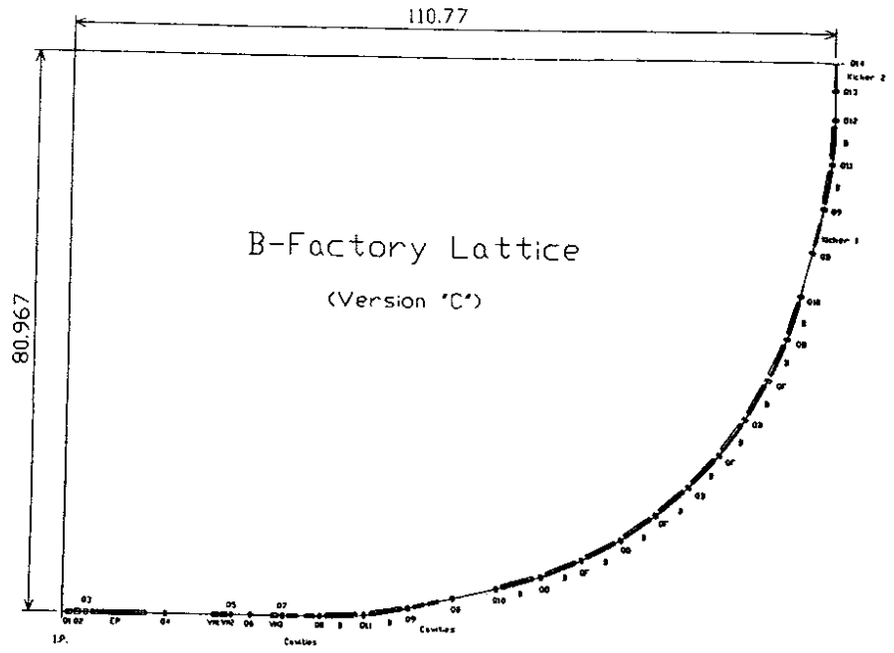

Figure 8: Quadrant of the magnetic structure of the PSI/SIN machine.

- A large beam-beam tune-shift ΔQ:

  A conservative assumption is $\Delta Q_{max} \approx 0.025$. Experience shows that with a careful aligment of the machine elements together with empirical orbit corrections ('golden orbit') and suitable feedback systems the space charge effects can be reduced. It seems possible to reach $\Delta Q_{max} \approx 0.05$.

Machine lattice: Following these design criteria together with some other constraints the machine lattice has been designed as shown in Fig.8. Properties of the lattice are:

- The injection can be done at the working energy, allowing for a refill without dumping the previous fill ('topping off'). This is a necessary condition for an efficient running of the machine with high average luminosity.
- The maximal β-function is everywhere, except in the mini-β quadrupoles, smaller than 30 m, as required for a large emittance.
- The dispersion vanishes in the interaction region, the RF cavities and the injection region.
- The dynamical and mechanical apertures are well matched by a suitable sextupole arrangement.

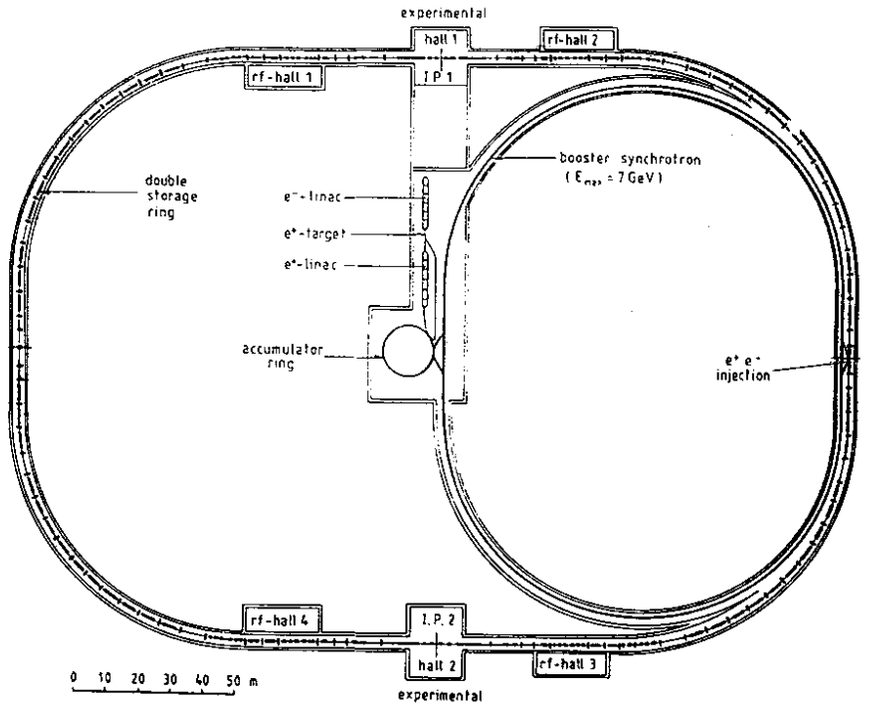

Figure 9: PSI/SIN B-factory.

- The free straight sections allow for the installation of a wiggler which can be used for tuning the emittance and as a synchrotron light source.

Injection system: A fast and effective injection is possible with a system consisting of a booster synchrotron, an accumulator ring and two linacs, one for electrons and one for positrons (Fig.9).

RF System: The RF system has to handle large beam loads of order 500 mA. Higher mode excitations in the cavities can be efficiently damped by employing cavities with low shunt impedance similar to superconductive cavities, but in a normal conductive version. The use of low shunt impedance, normal conductive cavities is possible because at such high currents the total power consumption is dominated by the beam load and not by thermal losses.

Interaction region: Subject of intensive development work is the beam separation scheme near the interaction region. One solution is the use of electrostatic separation plates. With a field of up to $3 \cdot 10^6 V/m$ over a length of 8 m the electron positron separation at the closest dipole magnet (VM1, Fig.10) will be 60 mm. The bending in this magnet is very weak (R =

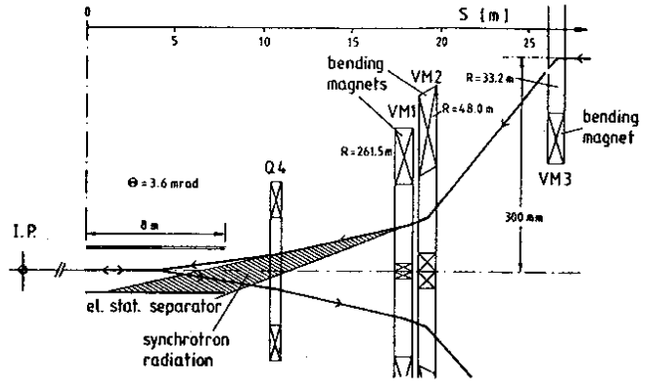

Figure 10: The vertical beam separation of the PSI/SIN B-factory.

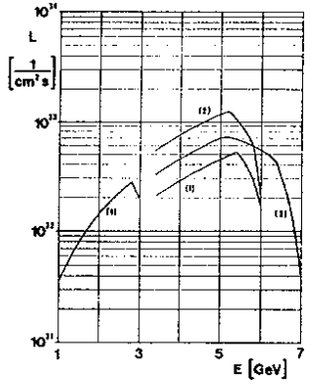

Figure 11: Luminosity curves for the **PSI/SIN B-factory**. The curves 2, 3, 4 are optimizations for different energies. The curve (2) represents the design goal.

261.5 m) so that a power of only 10 Watts/m is deposited by synchrotron radiation on the plates. Yet this causes cooling problems as the plates are on high voltage. As an alternative the use of RF magnets for the separation is investigated.

Luminosity: Figure 11 shows the expected luminosity as a function of the energy. The curves 2,3 and 4 are optimized for different energy ranges. Curve 2 represents the design value:

$$L(\Upsilon(4s)) \geq 10^{33} cm^{-2} s^{-1}$$

Schedule: The proposal for a machine and detectors has just been finalized. Together with the machine the construction of a new universal detector (see Sect.3) and a move of the Crystal Barrel detector to the B-factory (possibly in a later stage) is proposed. The approval is expected for the end of 1989, so that the construction could start in January 1990. The

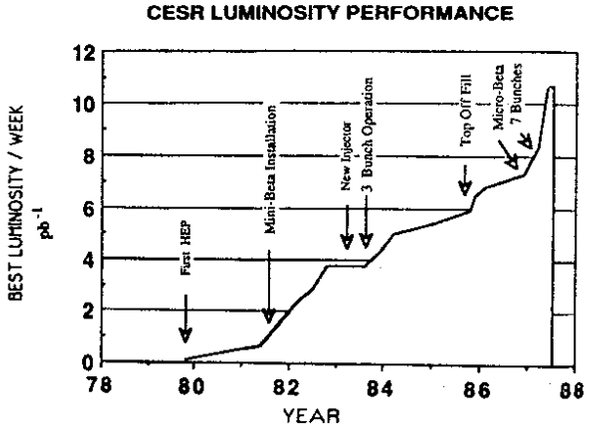

Figure 12: CESR's luminosity performance as a function of time showing the success of the upgrading program. From [9].

machine and the detector could then be commissioned in 1994. The costs are estimated to be around 170 million DM for both the machine and the detector. At present, contributions are expected from Germany and, at least on the detector side, from France. Other countries have signalled interest.

2.2.4 CESR Luminosity Upgrade

The storage ring CESR at Cornell has been continously upgraded since 1981 and the upgrading program still continues. Figure 12 shows the improvements of the average luminosity over the years. The most important steps in the upgrading program have been [9]:

- The installation of mini-β quadrupoles in 1981 reduced β_y^* from 9 cm to 3 cm and improved the luminosity by a factor 5 to $L = 1.6 \cdot 10^{31}\,cm^{-2}s^{-1}$.
- Multibunch operation has started in 1983. The bunches are separated outside the interaction regions by the socalled "pretzel orbit" scheme (Fig.13): electrostatic plates initiate oscillations of the reference orbit which are different for electrons and positrons. With an odd number of oscillations between the interaction regions one can achieve that the bunches cross only at the interaction points. The distance of the electrostatic plates to the interaction region determines the maximum number of bunches to be seven. However, problems with overheated RF windows required a reduction to three bunches.
- In 1986 small permanent magnetic quadrupoles were installed very close to the interaction region which made $\beta_y^* = 1.5$ cm possible.
- Improvement of the RF windows allowed in 1987 for the first time 7 bunch operation. With $\beta_y^* = 2$ cm a peak luminosity of $L = 5 \cdot 10^{31}\,cm^{-2}s^{-1}$ was reach yielding on average about 2 pb^{-1} per day and per detector.

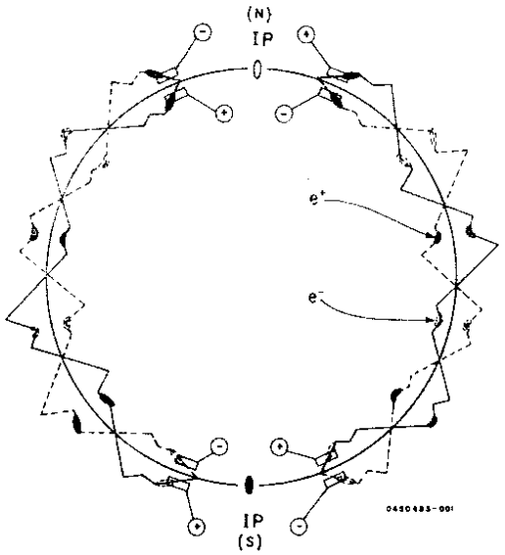

Figure 13: CESR's 'pretzel orbit' scheme.

Further improvements are planned to increase both the peak and the average luminosity [9]:

- Average luminosity gains are possible by a faster injection and improved reliability.
- The peak luminosity can be raised by higher bunch currents (11 mA) and reduction of the bunch length to 1.5 cm (allowing for smaller β_y^*).
- Appreciable gains are expected if the beams are collided in one interaction region only, in particular more bunches (14 per beam) with higher currents could be circulated.

If all improvements were independent, the luminosity could be increased by a factor of 20. This seems not to be quite likely but a luminosity of several times $10^{32}\,\mathrm{cm}^{-2}\mathrm{s}^{-1}$ may be possible.

2.2.5 Upgrade of the Tristan Accumulator Ring (AR)

A group of physicists in Japan has submitted a proposal to upgrade the Tristan Accumulator Ring (AR) as a B-meson factory and to construct a detector suited for B-physics in the threshold region [10]. The AR is presently used as an e^+e^- collider with a maximum energy of $\sqrt{s} = 11$ GeV and a design luminosity of $10^{31}\,\mathrm{cm}^{-2}\mathrm{s}^{-1}$ (Fig.14).

The upgrade is forseen to proceed in two steps:

- Until next year the luminosity will be increased in the single bunch mode by installing a micro-β scheme ($\beta_y^* = 2$ cm) and high emittance optics. For the latter change one exploits the fact that the horizontal emittance increases with a decreasing number of

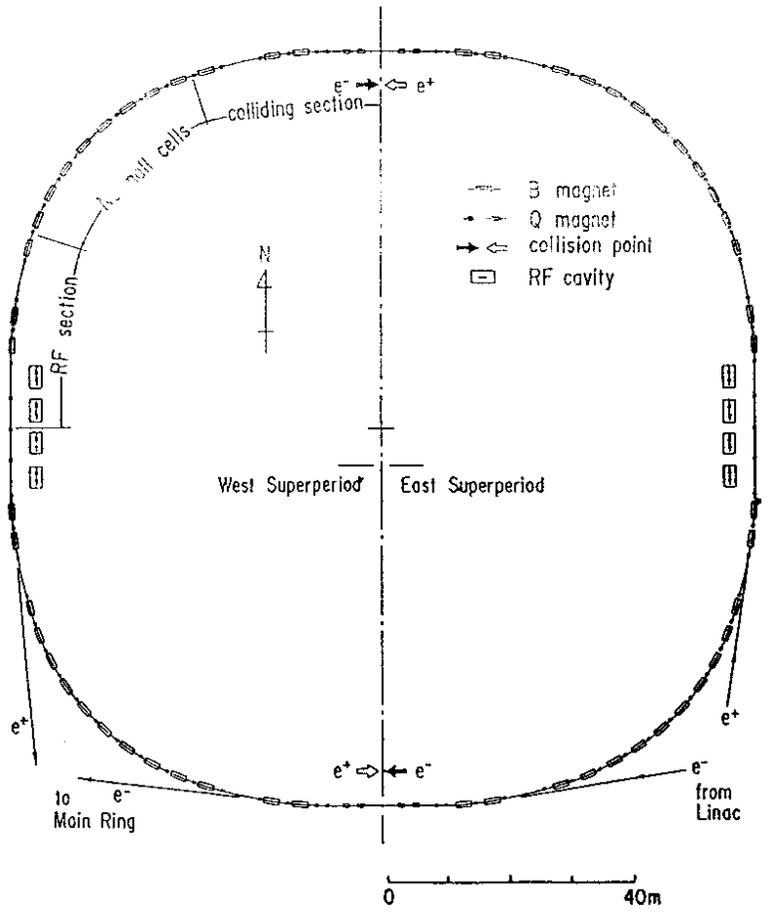

Figure 14: TRISTAN accumulator ring (AR).

betatron oscillations. Changing the tune from a phase advance of 90° per cell to 60° or 70° per cell will result in a 3 times larger emittance.

From these changes a luminosity of $L = 8 \cdot 10^{31}\,cm^{-2}s^{-1}$ at $\sqrt{s} = 11$ GeV is expected.

- In a second step multibunch operation is forseen, employing a 'pretzel orbit' scheme with electrostatic separators as developed for CESR. With four bunches per beam a luminosity increase by a factor 2 to 3 is possible yielding $L \approx 2-3 \cdot 10^{32}\,cm^{-2}s^{-1}$.

Although the peak luminosity of the AR may become similar to CESR the average luminosity probably will not, because the machine time has to be shared with synchrotron radiation users.

2.2.6 Asymmetric Machines

Motivation: The B-mesons produced at the $\Upsilon(4s)$ are nearly at rest ($\beta \approx 0.06$) with average decay lengths of about 20 μm. The decay products of the B and $\overline{B}$ are almost completely intermixed leading to a large combinatorial background for the reconstruction of exclusive final states (see also discussion in Sect. 1.3). Separating the decay products by associating them with two different decay vertices would increase the reconstruction efficiency by at least an order of magnitude. In addition, decay time dependent amplitudes which are relevant for mixing and CP- violation phenomena can be mesured. Note that direct CP-violation which is due to $B\overline{B}$ mixing vanishes if one integrates over all decay times.

Even with an optimal micro-strip vertex detector the B-decay vertices at the $\Upsilon(4s)$ cannot be separated on an event by event bases (see Sect.3.3). Therefore the idea came up to boost the B's by colliding electrons and positrons with different energies [21,16,17]. A boost with $\gamma\beta \approx 1$ increases the average B-decay length to about 400 μm, more comfortable for a vertex detector. Both B's are boosted along the beam direction so that there is no chance to reconstruct the primary vertex. However, detecting the decay length difference Δl is sufficient for disentangling the B's (the average Δl is equal to the average decay length). It also turns out that Δl is the proper variable which is sensitive to CP- violating asymmetries in decay amplitudes. Since B^0 and $\overline{B^0}$ can mix, there are two ways an initial B^0 can decay into a CP eigenstate f:

$$B^0 \rightarrow f \; and \; B^0 \rightarrow \overline{B^0} \rightarrow f\,.$$

The phase difference between both decay amplitudes is given by the Kobayashi-Maskawa phase. The interference between both amplitudes has a different sign for an initial B^0 as compared to a $\overline{B^0}$, generating an asymmetry in the decay rates. The asymmetry depends on the decay time difference Δt = t(B)- t($\overline{B}$) (Fig.15):

$$A = \frac{N(B) - N(\overline{B})}{N(B) + N(\overline{B})} \sim \sin \Delta m\, \Delta t\,.$$

Experimentally, one has to know if the initial state is a B^0 or $\overline{B^0}$. At the $\Upsilon(4s)$ the initial state can be tagged by measuring the C-parity of the recoiling particle.

The ARGUS group looked into the decays $B^0(\overline{B^0}) \rightarrow J/\psi K_s^0$. The CP eigenstate $J/\psi K_s^0$ has a very clean signature with the J/ψ decaying into a lepton pair and the K_s^0 into a pion pair (Fig.16). With about 100 $J/\psi K_s^0$ and a tagging efficiency of about 30% to 40% the CP-violating asymmetry could become measureable [22]. ARGUS has found 1 $J/\psi K_s^0$ event

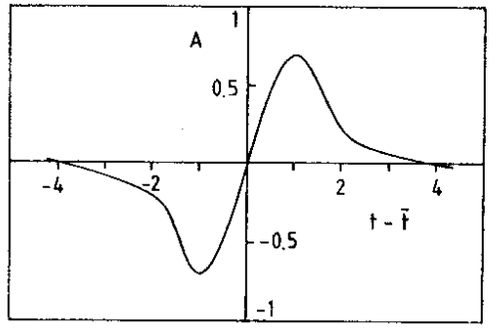

Figure 15: Expected asymmetry in the B^0 and $\overline{B^0}$ decay rates as a function of the decay time difference if the B^0 decays into a CP eigenstate.

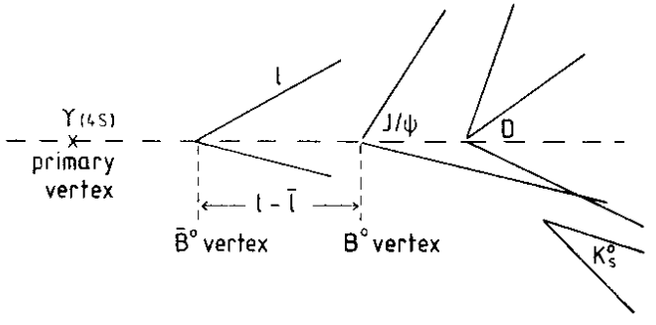

Figure 16: Vertex pattern for the CP violating decay mode discussed in the text as it could be observed in an asymmetric machine.

in an integrated luminosity of 100 pb^{-1}, suggesting that the luminosity of an asymmetric machine should be about two orders of magnitude larger than that of DORIS.

The "flying B's" scheme is somewhat uncomfortable for the particle detection: Due to the boost more particles are lost in the forward direction; the smaller angles under which the particles traverse the beam pipe cause more multiple scattering and less effective extrapolation from the vertex detector to the beam line. A detector design which could overcome these problems is under investigation [22]

In a machine operating at the $\Upsilon(4s)$ with beam energies of 2 to 3 GeV and 12 to 14 GeV the B's are boosted with $\beta\gamma = 0.7$ to 1.0. If the two beams have equal spreads σ_x^* and σ_y^* (whith $\sigma_x^* \gg \sigma_y^*$), the luminosity is estimated to be [16].

$$L = \frac{\pi\gamma_{cm}^2 f_b \Delta Q_1 \Delta Q_2 \sigma_x^* \sigma_y^*}{4r_e^2 \beta_{y1}^* \beta_{y2}^*}$$

f_b is the bunch crossing rate. The indices 1 and 2 refer to the two beams. In this formula the luminosity depends on the cms energy explicitely only via $\gamma_{cm}^2 = 4\gamma_1\gamma_2$, i.e. not on the specific beam energies. In [16] some reasoning is given that the tune shifts ΔQ_1 and ΔQ_2 may as well not depend on the energies or the other beam parameters and may have similar limits as in symmetric machine. Problematic is the focussing of the two beams with very different energies. Independent mini-β optics for each beam requires a beam separation very close to the interaction point which may swamp the detector with synchrotron radiation.

An asymmetric e^+e^- collider has been studied at DESY [17] and SLAC [16]. At DESY it was suggested to run PETRA at 14 GeV in combination with a new smaller ring (L = 115.2 m). With 20 PETRA bunches and one bunch in the small machine the luminosity is estimted to be $10^{32}\,\mathrm{cm}^{-2}\mathrm{s}^{-1}$. In a similar study for running PEP together with a new small ring a luminosity of $5 \cdot 10^{32}\,\mathrm{cm}^{-2}\mathrm{s}^{-1}$ is estimated [25]. Instead of two rings one could also think of a linac - ring combination [26].

Further investigations have to find out if these ideas can be realized. In particular, one has to study if the synchrotron radiation background in the interaction region can be controlled and if a detector can be constructed which fully exploits the advantage of separated decay vertices.

2.3 Linear Collider B-Meson Factories

2.3.1 Machine principle and luminosity limitations

In a storage ring the charge density in a bunch is limited by instabilities caused by the beam-beam interaction. This type of instability does not occur in e^+e^- linear colliders where the beam particles are used only once and thus the luminosity yield per bunch crossing can be made much larger. The basic luminosity formula

$$L = \frac{N_+ N_- f}{4\pi\sigma_x\sigma_y} \qquad (10)$$

implies that the maximum luminosity is obtained for:

- the highest number of electrons or positrons per bunch which can be accelerated without diluting the emittance,

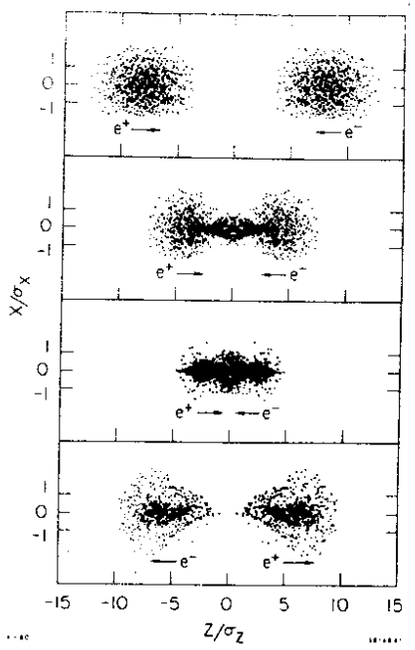

Figure 17: Pinch effect (from [19]).

- the smallest emittance which can be obtained employing damping rings before the acceleration,
- the highest possible focussing which determines together with the emittance the beam size (of order 1 μm) in the interaction point,
- the highest pulse repetition rate.

In linear colliders the mutual focussing of the bunches leads to an effective decrease of the transverse beam size during the crossing and thus to a luminosity enhancement (pinch effect, Fig.17). The strong focussing is followed by a disruption of the beam. The pinch effect enhancement is usually expressed by an additional factor H in the luminosity formula (10). H depends on the disruption parameter D which measures the number of oscillations of the particles during the bunch crossing and which is proportional to the bunch length. For increasing D the enhancement H is expected to saturate (disruption limit) and for D $\geq$ 10 plasma instabilities may even reduce the luminosity. Since D is proportional to the longitudinal bunch length it is important to have short bunches. On the other hand, the stronger focussing implied by a short bunch length (for a given number of particles per bunch) causes larger radiation losses during the crossing ('beam-strahlung'). This results in an energy spread which grows with shorter bunches:

$$\frac{\sigma_E}{E} \sim \frac{1}{\sigma_l^2}.$$

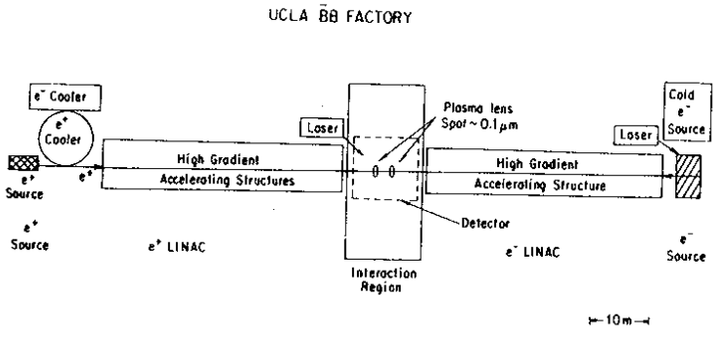

Figure 18: The UCLA normal conducting linear collider B-factory.

Keeping a small beam spread, as required for resonance running, has therefore a negative effect on the luminosity.

Colliding the beams in a micrometer spot poses severe requirements on the stability and the optical properties of the focussing system. Whether these requirements can be met and whether the theoretical calculations on the beam dynamics are realistic, may become clear from the experience gained in operating SLC. The design luminosity of SLC is about 3 to 4 orders of magnitude below that required for a B-factory. The higher luminosity can only be obtained if major technical improvements can be achieved for

- the final focus system,
- high intensity electron and positron sources,
- high power RF generators for normal conducting cavities,
- higher accelerating field gradients in superconducting cavities.

Research and development work for linear collider B-factories has been started at UCLA [14] and Frascati [13].

2.3.2 The UCLA project

The concept of the UCLA B-factory (Fig.18) has the main features:

- a high gradient normal conducting accelerating structure (>150 MV/m)
- power supplied by a relativistic klystron;
- a repetition rate of about 1 kHz;
- positron production by "non-conventional techniques" (yet to be developed);
- a submicron beam spot of about 0.1 μm achieved by a plasma lense (Fig.19).

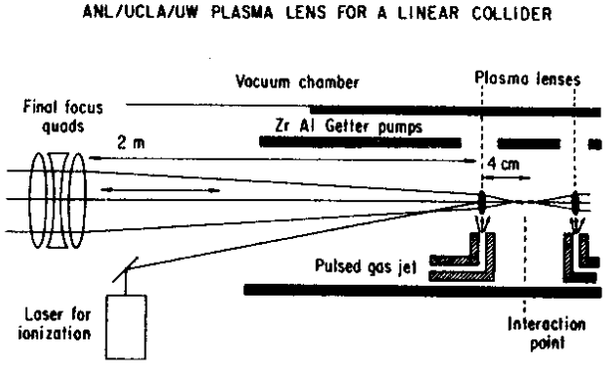

Figure 19: Use of a fully ionized gas beam as a strongly focussing lense in a linear collider.

- a large disruption parameter (little know about beam dynamics);
- a modest energy spread (about 40 MeV at the $\Upsilon(4s)$).

If all works the luminosity could reach

$$L = 4 \cdot 10^{34} cm^{-2} s^{-1}$$

corresponding to more than 10^8 $B\overline{B}$ pairs per year. With the high gradient the whole machine would be relatively short fitting into available space on the UCLA campus.

2.3.3 The Frascati project

The Frascati project [13] is described in detail by G. Coignet in his lecture at this meeting. For completeness I just show a picture of the proposed machine ARES (Fig.20). The machine is based on two superconducting linacs with a recirculation scheme. Recirculation is necessary because the energy gain will only be 1.05 GeV over the 500 m linacs corresponding to effectively 2 MV/m. While this is much worse than for normal conducting structures, the linacs can supply nearly continuous currents. The machine can be used for different purposes, as a B-factory at the $\Upsilon(4s)$ the luminosity is estimated to be about $10^{34}\,\mathrm{cm}^{-2}\mathrm{s}^{-1}$.

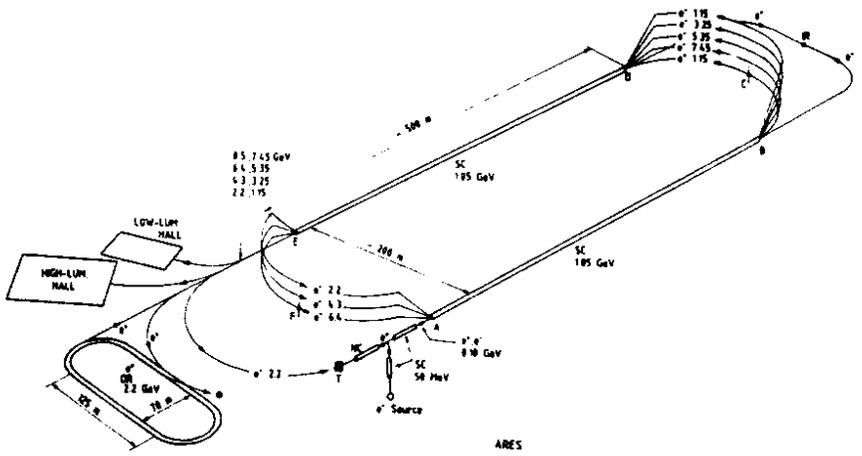

Figure 20: The racetrack superconducting linacs at Frascati (ARES project).

3 B-Factory Detectors

3.1 Detector Requirements

The gain in luminosity has to be accompanied by improvements in the detector capabilities. The overall efficiency of an experiment can be increased substantially, if currently available detector techniques are fully exploited.

Aiming at an increase of the reconstruction efficiency for B's from currently about 10^{-3} to about 10^{-2} the following detector properties are particularly important:

- charged track reconstruction with high momentum resolution and high efficiencies down to low transverse momenta;
- vertex detection with resolutions in the 10 μm range;
- γ and electron detection with high resolution and high efficiency down to small energies;
- particle identification for electrons, muons, pions, kaons and protons up to the highest momenta occuring in B-decays.

Common to all detector components are the requirements:

- large solid angle coverage;
- trigger and data acquisition suited for high luminosity and high bunch crossing rates.

It is generally agreed on that any new detector for B-physics has to be at least as good as the upgraded CLEO-detector, CLEO II [3], which is right now being installed. Figure 21 shows the detector with the following main components: Charged particles are detected in a vertex detector (based on the drift chamber principle) and in the main driftchamber which, provides also dE/dx information for particle identification. Additional particle identification is obtain from a time-of- flight system. The CsI crystals of the calorimetry are placed inside the superconducting coil. The whole detector is surrounded by a muon detector. Parameters of the detector are listed in Table 5 in comparison with the ARGUS detector and the proposed AR detector [10]. It is obvious that the ARGUS detector will not be competetive with CLEO II. The AR detector in Fig.22 particularly emphazises particle identification employing dE/dx, from the drift chamber, TOF from planar spark counters (PSC) and ring imaging Cerenkov counters (RICH).

Figure 23 shows the detector proposed for the PSI B-factory [12]. The detector components are from inside to the outside: a micro- strip vertex detector, drift chambers, RICH counters, a CsI- calorimeter, the superconducting coil and a muon detector. The important new features are the micro-strip vertex detector and the RICH counter. The use of these two technologies is expected to yield an essential step in performance compared to existing B physics detectors.

	AR	CLEO II	ARGUS
Magnet			
Coil size	$2.9m^{\phi} \times 2.8m^{l}$	$3.1m^{\phi} \times 3.5m^{l}$	$2.8m^{\phi} \times 2.9m^{l}$
Field (Tesla)	1.5	1.5	0.8
Central DC			
Rin(cm)	17.0	17.78	15.0
Rout(cm)	74.0	94.7	85.9
Lever arm(cm)	~ 50	~ 71	~ 64
layers(stereo)	45(21)	51(11)	36(18)
sense wires	11,904	12,240	5.940
gas (1 atm)	CO_2-isobutane	Ar-Ethane	Propane
resolution ($\sigma\mu$m)	100	150	150
$\Delta p_T/p_t(\%)$	$\sqrt{(0.28p_t)^2 + (0.50)^2}$	$\sqrt{(0.24p_t)^2 + (0.5)^2}$	$\sqrt{(0.65p_t)^2 + (0.45)^2}$
dE/dX (FWHM)	16%	14%	10.4%
Cherenkov	RICH		
	R=74-92cm		
	K/π sep.($> 3\sigma$)		
	for p=0.8-3 GeV/c		
TOF	PSC	Scinti.	Scinti.
R(cm)	92-101	96	96
number: barrel+ends	288+2 x 80	64+2 x 32	64+2 x 48
σ(ps)	50	150	220
max.mom. of 3σ			
separation for K/π	1.4 (GeV/c)	0.8	0.6
EM cal.			
min.radius(cm)	100	102	95
material	CsI(Tl)	CsI(Tl)	Pb-scinti.
thickness[X_0]	15	16	12.5
readout	Photodiode	Photodiode	PMT
channels:barrel+ends	6400+2×850	6144+2×840	1280+2× 240
σ/E(% (E in GeV))	$2.1/E^{1/4} + \text{const}$	$\sqrt{(2 + 2/\sqrt{E})^2 + (0.2/E)^2}$	$\sqrt{(8/\sqrt{E})^2 + 7^2}$
e/π sep.	10^{-3}	10^{-3}	10^{-2}

Table 5: Parameters of the AR, CLEO-II and ARGUS detectors. From [10].

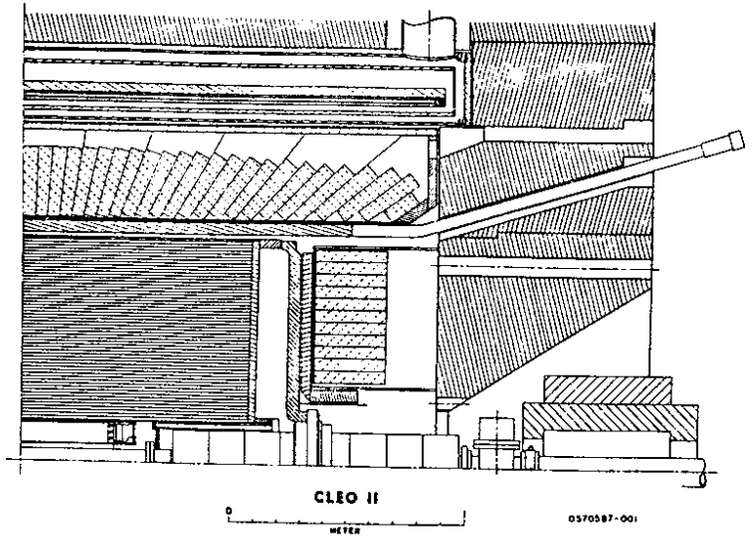

Figure 21: Quadrant of the CLEO-II detector.

3.2 Charged Particle Tracking

In all proposed B-factory detectors charged particle tracKing will be done by some type of a drift chamber. Important requirements on such a device are

- good momentum resolution down to low momenta;
- high track detection efficiency down to low momenta;
- provision of dE/dx information;
- provision of a fast trigger.

Momentum resolution: If a track, which is bend by a magnetic field B, is measured over a length L by N equally distributed points the resolution of the momentum transverse to the B-field is [27]:

$$\left(\frac{\sigma_{pt}}{p_t}\right)^2 = \left(\frac{p_t \cdot \sigma_\phi}{0.3 \cdot B \cdot L^2}\right)^2 \frac{720}{N+5} + \frac{0.0036}{B^2 \cdot L \cdot \beta^2 \cdot X_0 \cdot \sin\theta}. \quad (11)$$

The first term contains the spatial resolution of the detector which measures azimuth angles ϕ at fixed radii. Optimization of this term yields the requirements:

- Good spatial resolution: about 100 μm can be reached.
- High B field: most designs provide a superconducting coil generating 1.5 Tesla.

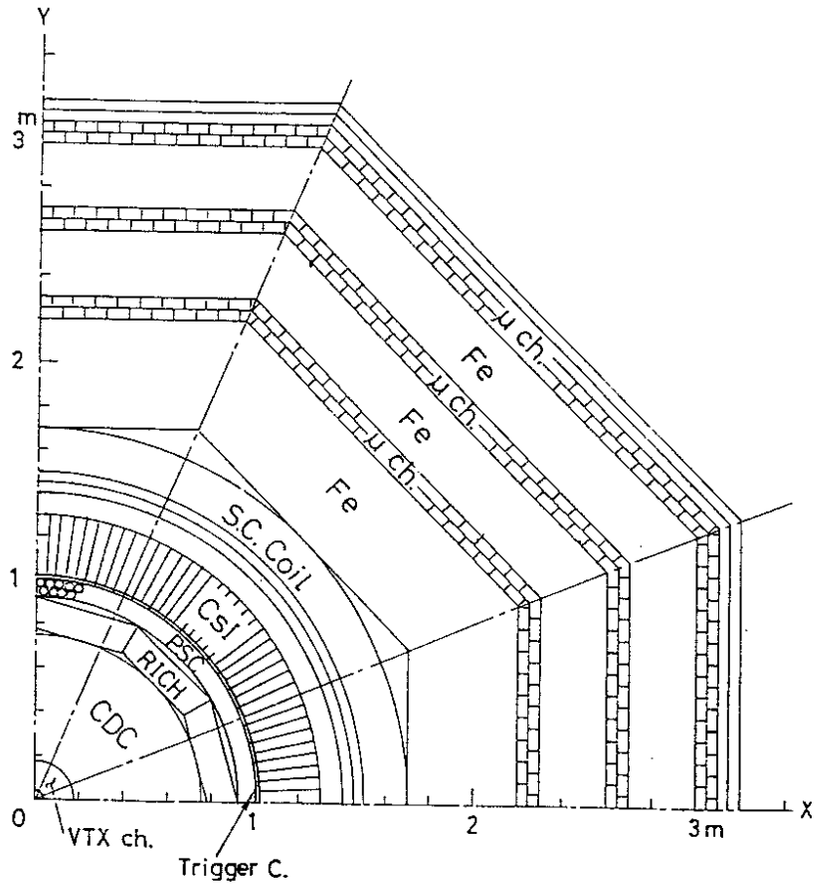

Figure 22: Detector proposed for the TRISTAN Accumulator Ring (AR).

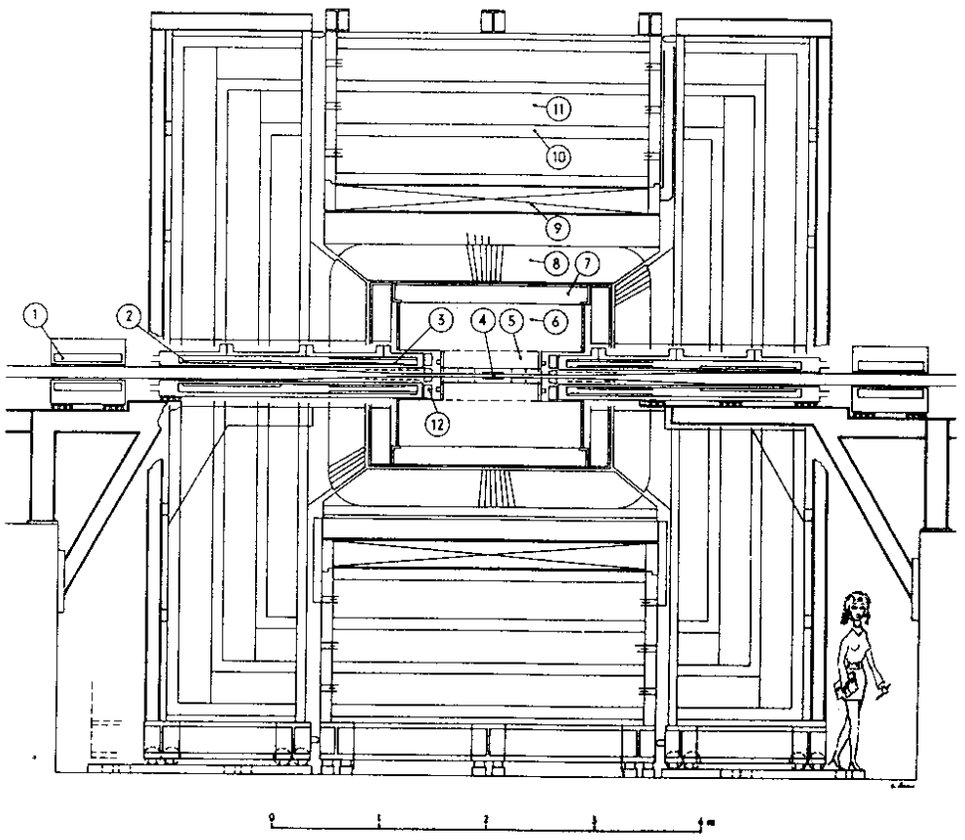

Figure 23: Detector proposed for the PSI/SIN B-Factory.
(1) Quadrupole Q3, (2) and (3) minibeta quadrupoles Q1 and Q2, (4) Silicon Vertex Detector, (5) Precision Tracking Chamber, (6) Main Tracking Chamber, (7) RICH, (8) CsI Calorimeter, (9) Coil, (10) Muon Chambers, (11) Iron, (12) Forward Calorimeter, (13) support of inner detector, (14) rails for CsI support.

		BMF1	BMF2	BMF3
D Mass Resolution (MeV)	Multiple scattering(gas)	6.13	5.38	4.49
	R_ϕ resolution	7.19	3.63	2.26
	z resolution	3.93	2.72	2.09
	Multiple scattering(beam pipe)	2.37	2.37	2.37
	$\sqrt{\Sigma(total)^2}$	10.50	7.43	6.28
	With all Effects	11.14	7.77	6.59
$D^* - D$ Mass Resolution (MeV)	Multiple scattering(gas)	0.289	0.283	0.280
	R_ϕ resolution	0.213	0.184	0.170
	z resolution	0.264	0.225	0.203
	Multiple scattering(beam pipe)	0.494	0.494	0.494
	$\sqrt{\Sigma(total)^2}$	0.665	0.639	0.627
	With all Effects	0.588	0.574	0.566

Table 6: Mass resolutions for different tracking detector designs.

- Large track length in the tracking detector: The most stringent limitation on L comes from the costs of the outer detector parts as the costs increase more than quadratically with the radius of the tracking chamber. Therefore the size of the tracking chambers will always be a compromise, in particular if space has also to be provided for Cherenkov counters.

The second term in (11) is due to multiple scattering if the track traverses $X_0 \sin\theta$ (θ = dip angle) radiation lengths. Since the average momenta in B-decays are only about 400 MeV it is crucial to minimize the amount of material the track passes through. Studies for the proposed ARES detector (Frascasti) [28] suggest that a low Z gas, such as a He-DME mixture, would yield much better resolutions even at higher momenta than with standard gases (argon, CO_2 etc.). This is not generally agreed on and certainly higher Z gases provide better dE/dx information.

As a specific example Table 6 shows for different detector designs the D^0 mass resolution in B-decays for the decay $D^0 \to K^-\pi^+$ and the resolution of the $D^* - D^0$ mass difference. Without going into the details of the different detector models in the table, let us note that BMF1 corresponds approximately to the performance of CLEO II and BMF3 to that of the proposed PSI/SIN detector. It is obvious that the resolution of the $D^* - D$ mass difference is dominated by multiple scattering in the beam pipe (including the vertex detector). This is due to the low momentum pion in the transition

$$D^* \to \pi D. \qquad (12)$$

Preliminary studies showed that a significant improvement for the resolution can be achieved if the angular measurement is taken from the precision vertex detector while the momentum is determined in the outer drift chamber [29].

Efficiency at low momenta: B-mesons predominantly decay via charmed mesons and a large fraction of it via D*'s. Therefore it is extremely important to have a high efficiency for

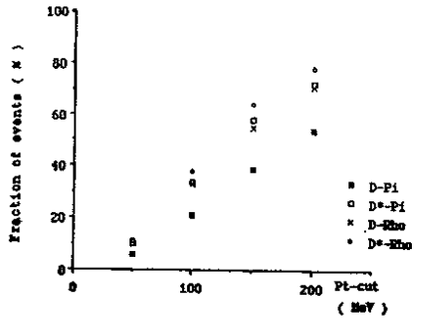

Figure 24: Event loss due to lower p_T-cut for charged particles.

D* reconstruction, which in turn requires a good detection efficiency for the low momentum pion in (12). Figure 24 shows the event losses due to different p_T cuts for some selected final states. Efficiencies of more than 90% down to 30 MeV/c are desireable.

Since 30 MeV/c tracks curl up in a 1.5 Tesla field with a maximum distance of about 7 cm from the beam it is necessary to have good track measurements with efficient pattern recognition close to the beam pipe (which is assumed to have radii of only about 1.5 cm, see next section on vertex detectors)

dE/dx measurement: A drift chamber naturally provides a large statistics sample of ionisation measurements which should be used to support particle identification in the low momentum range.

Fast tracking trigger: Those B-factories which are designed as multibunch storage rings have to handle bunch crossing rates of up to 10 MHz. In order to keep the dead time low the background has to be rejected stepwise by a multilevel trigger scheme. The first level trigger has to come very fast, within the time between bunch crossings. At a B-factory the first level trigger will mainly be based on a fast track trigger selecting tracks coming from the interaction region. The most effective background reduction is expected from a vertex recognition in the r-z plane, i.e. along the beam. Unfortunately, fast r-z measurements are not easily obtained and require some additional attention in the chamber design (e.g. cathode strips).

3.3 Vertex Detectors

B and D mesons and τ leptons are weakly decaying with lifetimes of order 10^{-12} sec, corresponding to decay lengths of order 100 μm in the Υ energy range (Fig.25). The average decay lengths of B, D and τ particles from $\Upsilon(4s)$ decays at rest (symmetric machine) are listed in Table 7.

A vertex detector with a 10 μm resolution of the vertex allows to study

- lifetimes and
- mixing patterns including CP violating effects.

particle	$c\tau$ [μm]	l($\Upsilon(4s)$) [μm]
D^0	130	60
$D^{\pm}$	280	115
B	430	25
τ	100	280

Table 7: Average decay length of different particles at the $\Upsilon(4s)$.

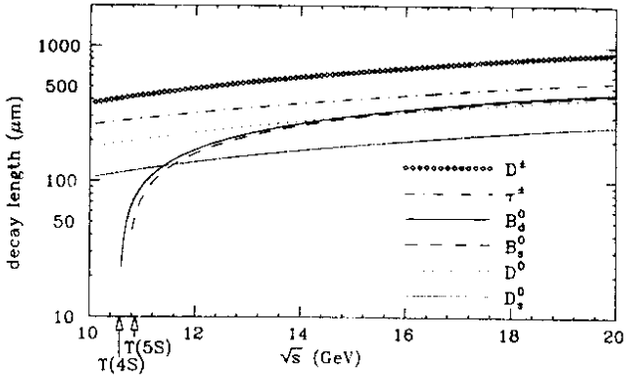

Figure 25: Average decay lengths for different particles as a function of the event energy. From [30].

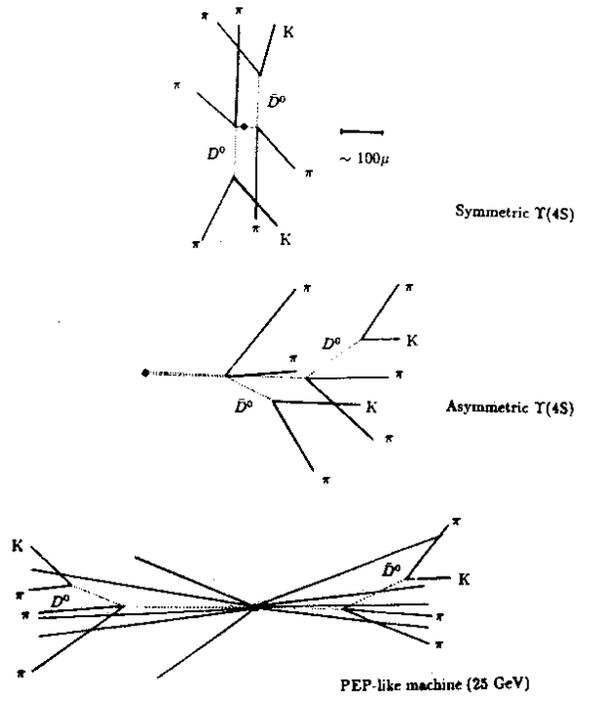

Figure 26: The **decay $B^0 \to \overline{D^0}\pi^+\pi^-$, $\overline{D^0} \to K^+\pi^-$ and its charge conjugate** as seen in different machines. From [31].

While in the case of B-mesons produced at the $\Upsilon(4s)$ without boost such measurements would be rather marginal, an asymmetric machine with ' flying B's ' is better off (see Fig.26 and Sect.2.2.6). In both cases the B reconstruction efficiency can be appreciably increased by combining particles which are coming from a common vertex. In this way especially the charmed particles can be removed from the combinatorics.

The best vertex resolutions are obtained with solid state detectors such as micro-strip or CCD detectors [30]. However, until recently the standard thickness of Si-strip detectors was 300 μm and only one coordinate measured per layer. Now it appears possible to get 170 μm wafers (or even less) with double sided read-out. For the application of micro-strip detectors in B-factories the minimization of material is most crucial because of the low average momenta of about 400 MeV. For the design of the new ARGUS micro vertex detector which will be installed at the beginning of 1989 a gaseous detector technique still appeared superior over Si-strip detectors. With the development of thin wafer techniques the conditions definitely change. This becomes clear from Fig.27 where the impact parameter resolutions of the ARGUS micro vertex drift chamber is compared to thin Si-strip detectors. For the strip detectors it was assumed that two layers are sufficient. This requires that the vertex detector hits can be associated to the tracks extrapolated from the outer tracking devices

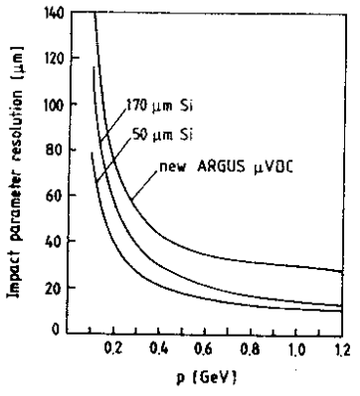

Figure 27: Impact parameter resolutions for the new ARGUS micro vertex drift chamber (r_{min} = 26 mm, beam pipe: 500 μm beryllium) and two-layer micro-strip vertex detectors with a thin front layer (r = 17 mm, 190 μm beryllium.)

with sufficient acuracy (50 to 100 μm).

For the PSI/SIN detector [12] a two layer Si-strip detector is proposed (Fig.28). The detector will be built as a self-supporting polygonal structure around a thin beryllium beam pipe (thickness 190 μm, radius 15 mm). The thin wafers are connected by bonds with a dead space of only about 450 μm at each corner. The highly integrated readout electronics is placed on one narrow rim.

The success of the vertex detectors sensitively depends on the thickness of the beam pipe and the distance from the interaction point (the vertex resolution deteriorates linearly with the lever arm for the extrapolation). Here linear collider machines have an advantage as narrow beam pipes are possible and as the beam spot itself is defined with a micron precision. The proposed vertex detector for the ARES detector at the Frascati linear collider is shown in Fig.29 [28]. The minimal detector radius is 1 cm.

Performance studies for the PSI/SIN vertex detector show that D vertices can be reconstructed with resolutions of 24 μm parallel and 12 μm perpendicular to the line of flight of the D. The corresponding numbers for B decays with a sufficient number of charged tracks are 12 μm and 16 μm, respectively, which is somewhat below the average decay length of B's ($\sim$ 25 μm). This suggests that in favourable situations even the $B - \overline{B}$ separation may be possible with a micro-strip detector.

3.4 Particle Identification

Particle identification and vertex detection are the two aspects of B-factory detectors which need most technical development work and where improvements may be most rewarding. The positive effect of particle identification up to high momenta is demonstrated in Fig.30 for the decay $D^0 \to K^-\pi^+$.

To set the scale we give a list of requirements for particle separation as worked out for the PSI/SIN detector:

- electron-hadron: 1000:1 for p > 0.5 GeV (dE/dx, calorimetry, RICH)

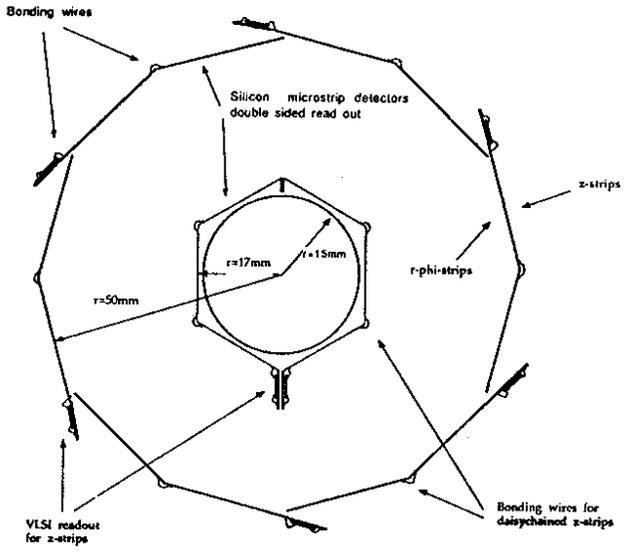

Figure 28: Silicon strip vertex detector proposed for the PSI/SIN B-factory.

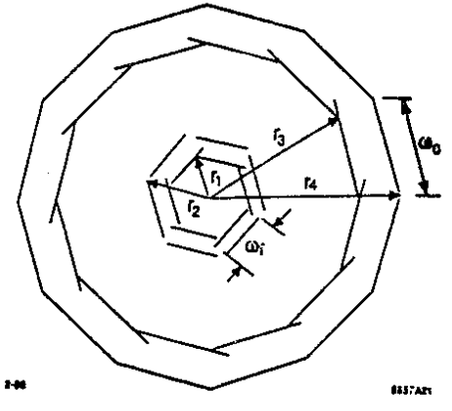

Figure 29: Silicon strip vertex detector proposed for the ARES B-detector.

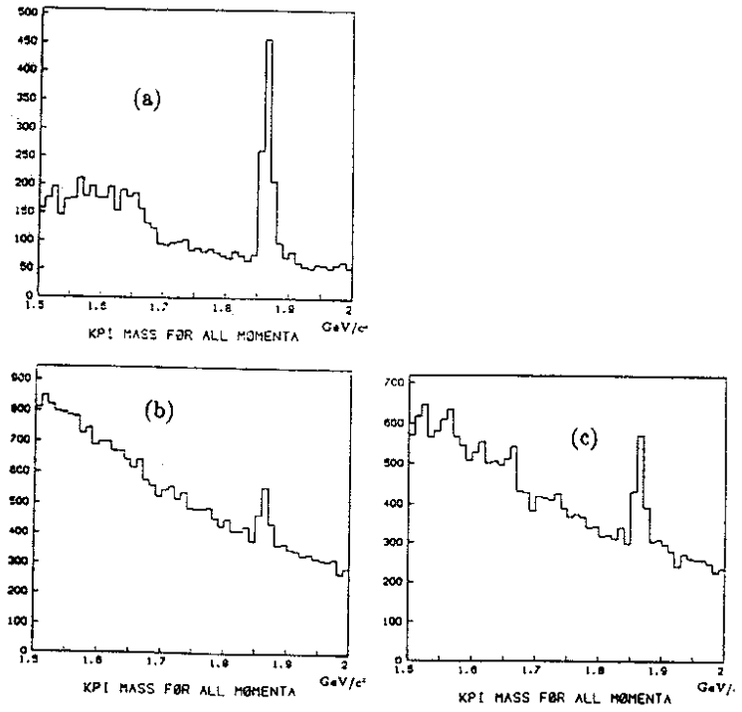

Figure 30: Example for the reduction of combinatorial background by particle identification. The D^0 signal in the $K^-\pi^+$ mass distribution is shown for (a) the full particle identification as expected for the AR detector, (b) no K/π separation and (c) K/π separation up to 0.8 GeV/c.

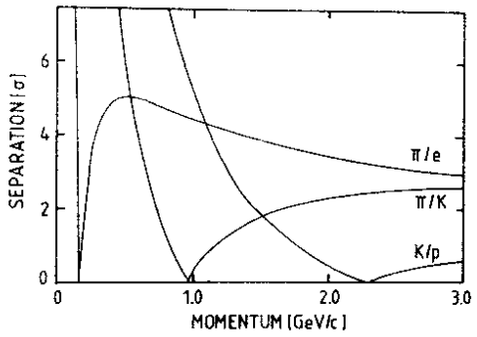

Figure 31: Particle separation by dE/dx measurement expected for the main drift chamber of the PSI/SIN detector.

- μ-hadron: 100:1 for p > 1 GeV (absorber and μ-chambers)
- π^0-γ: up to 5 GeV (calorimeter)
- π-K-p: up to 3 GeV (RICH + dE/dx + TOF)

Pion-kaon-proton separation is in B-experiments usually done be ionisation measurements in the central drift chamber and by time-of-flight measurements in fast scintillation counters. Both techniques are limited to low momenta, for π/K separation to about 1 GeV (Fig.31). A major step forward is expected from the use of ring imaging Cherenkov counters. These devices can be installed between the tracking chamber and the calorimeter covering a solid angle similar to the other detector components. Figure 32 shows the design for the PSI/SIN detector. Between the radiator and the photon detector the Cherenkov ring has to develop in a free space, resulting in an overall thickness of the detector of at least 20 cm. This additional radial space has an important impact on the size of the tracking chamber and for the cost of the calorimeter. The expected particle separation as a function of the momentum and polar angle is plotted in Fig.33. π/K/p separation is possible with better than 4 σ over the whole momentum range relevant for B-physics ($p_{max} \approx M_B/2 \approx 2.5\,GeV$).

3.5 Electromagnetic Calorimetry

An electromagnetic calorimeter in a B-factory detector has the following tasks:

- energy and direction measurement of photons (including photons from π^0),
- electron-hadron separation,
- fast trigger

Since on average about 30% of the total energy goes into photons with an average multiplicity of 8 (equal to the average charged multiplicity) the calorimeter should have optimal properties:

- a resolution of order $1\%/\sqrt{E}$;

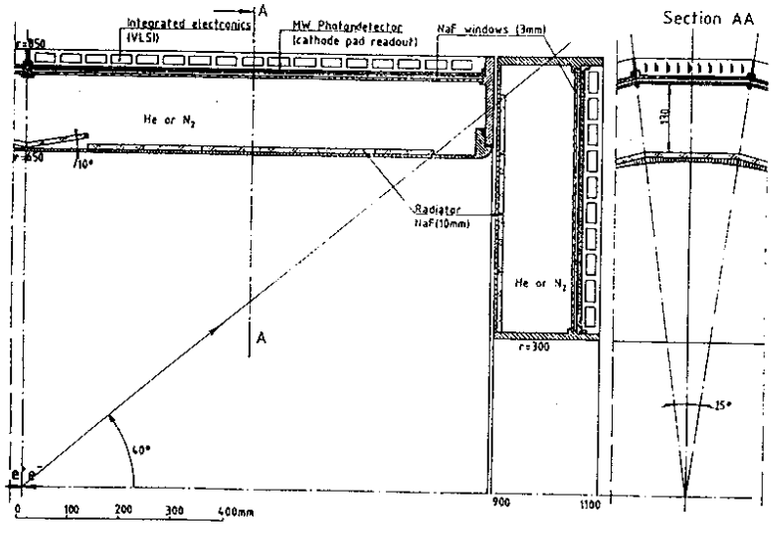

Figure 32: RICH counter design for the PSI/SIN detector.

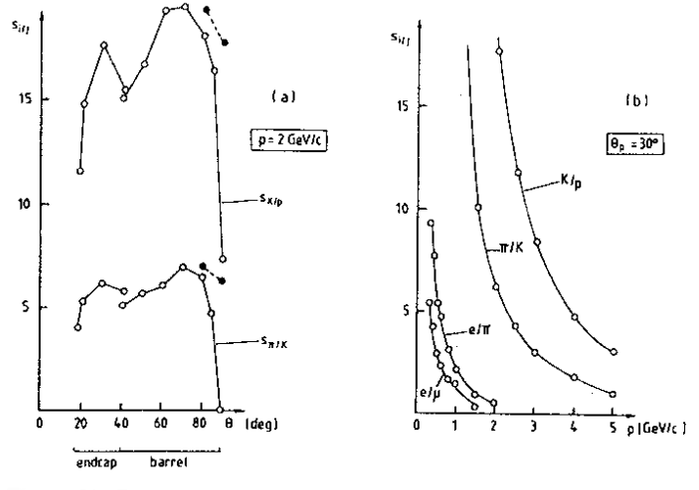

Figure 33: Particle separation in the proposed PSI/SIN RICH counter.

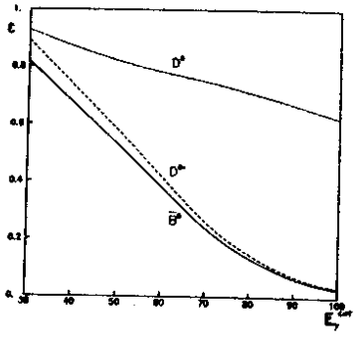

Figure 34: Dependence of reconstruction efficiencies on the lower photon energy cut (calculated for the ARES detector).

- high photon detection efficiencies down to the 10 MeV region;
- good angular resolution (fine granularity for π^0-γ separation up to about 5 GeV);
- little dead material.

The dependence of the B and D reconstruction efficiencies on the photon energy cut is shown in Fig.34, demonstrating the importance of high detection efficiencies at low energies.

There is clearly a conflict between the demands for high photon detection efficiencies and good particle identification. With about 0.15 X_0 a RICH counter reduces the detection efficiency of a 100 MeV photon by nearly 10%. In this respect it is not clear if the planar spark counters in the AR detector (PSC, Fig.22) with 0.29 X_0 are really improving the overall detector performance.

The requirements on a B-factory calorimeter can only be met by anorganic scintillating crystals such as CsI(Tl), BGO, BaF_2 and others (NaI is difficult to handle because of it hygroscopicity) [34]. Scintillating glas is an interesting alternative [33]. However, its low light yield of about 400 γ's per MeV is, e.g., about two orders of magnitude smaller than for CsI(Tl) limiting the use of photodiodes in magnetic fields.

Following the CLEO II detector, a CsI(Tl) calorimeter is also proposed for the AR and PSI/SIN detectors, while BGO is proposed for the ARES detector. The PSI/SIN calorimeter will have about 12000 crystals each 18 radiation lengths deep yielding the following energy and angular resolutions.

$$\left(\frac{\sigma_E}{E}\right)^2 = \left(0.01 + \frac{0.01}{\sqrt{E}}\right)^2 + \left(\frac{0.001}{E}\right)^2$$

$$\sigma_\Theta = \frac{4\,mrad \cdot \cos\Theta}{\sqrt{E}}$$

$$\sigma_\Phi = \frac{4\,mrad}{\sqrt{E}}$$

The three terms in the energy resolution formula are due to leakage, photon statistics and electronic noise, respectively. The resolutions for electromagnetic showers translate to a π^0

mass resolution of 2% at 1 GeV. The combined calorimeter, dE/dx and RICH measurements yield an electron-hadron separation of 1000:1. The granularity assures that in about 80% of the $\Upsilon(4s)$ events all showers are completely separated.

4 Concluding Remarks

It has not to be stressed again that B-meson physics, or more generally the physics of the third fermion family, adresses fundamental questions. The e^+e^- annihilation in the Υ energy range is in many respects most suited for this type of research as it has been demonstrated by the CESR and DORIS experiments. In other energy ranges, e.g. e^+e^- collisions at the Z^0, or at other machines, e.g. pp colliders, b-quark physics is more difficult due to lack of luminosity and/or efficiency. At threshold energies major progress can only be made with much higher luminosity machines and detectors which have much higher reconstruction efficiencies, in particular for B-mesons.

In the early nineties, Europe needs a new machine with new detectors as a powerful counterpart to the upgraded CESR machine and the CLEO-II detector. In such an important field of research an experiment certainly should not be left without a healthy competition.

The costs for a B-meson factory (at least with conventional techniques) are low compared to other projects currently pursuit. While linear collider B-factory projects are very interesting and necessary developments their time scale probably extends more to the year 2000. For the near future a storage ring concept is most promising to be realized. The PSI/SIN B-factory could supply beams for experiments in 1994 provided approval comes in 1989. DESY certainly has a high interest in continuing its successful B-physics program. The considered asymmetric machine could be regarded as complementary to the PSI/SIN machine. A machine which offers a realistic chance to discover CP-violation in the B-system should certainly get a high priority.

Acknowledgements: I am grateful to the many colleagues which provided me with all the informations I needed to prepare these lectures. In particular, I like to mention R. Eichler, K. Schubert and K. Wille. I also want to thank my colleagues in the ARGUS collaboration which gave me, as a late-comer into the group, the chance to get some insight into the beauty of B-physics. Finally, let me thank the organizers of this interesting and stimulating meeting which took place in a pleasant atmosphere.

This work was supported by the German Bundesministerium für Forschung und Technologie under contract number 0234DOAI.

References

[1] ARGUS Coll., H.Albrecht et al., Phys.Lett. 192B (1987) 245.

[2] A.Fridman, Some Physics Motivations for a B-Meson Factory, Proc. of the Workshop on Future of B Physics, Saclay, March 1987.

[3] Updated Proposal for Improvements to the CLEO Detector, CLNS 85/634, 1985; E.Nordberg, The CLEO II Detector, CLNS 87/94.

[4] A.Fridman, B-Physics with pp Colliders, Proc. of the B-Meson Factory Workshop, Stanford, Sept. 1987.

[5] R.A.Eichler and Z.Kunszt, Charm, Bottom and Top Production in High Energy Electron Proton Collisions, ETHZ-IMP P/88-1 (subm. to Nucl.Phys.B).

[6] R.D.Peccei, B Physics and CP Violation at UNK, Proc. of the Workshop on the Experimental Program at UNK, Protvino, Sept. 1987 (DESY 87-134).

[7] J.L.Rosner, A.I.Sanda and M.P.Schmidt, Proc. of the Workshop on High Sensitivity Beauty Physics at Fermilab, Batavia, Nov. 1987.

[8] R.Eichler, K.R.Schubert and K.Wille, Storage Ring or Linear Collider as a B-Factory, SIN-BFP/87-4.

[9] D.L.Rubin, CESR Luminosity Upgrade, Proc. of the UCLA Workshop 'Linear Collider $B\overline{B}$ Factory Conceptual Design', Los Angeles, 26-30 Jan. 1987;
K.Berkelman, The Future Cornell Program or CESR as a B Factory, B-Meson Factory Workshop, SLAC, Sept.1987 (CLNS 87/101).

[10] F.Abe et al., Proposal for Study of B Physics by a Detector with Particle Identification and High Resolution Calorimetry at TRISTAN Accumulator Ring, KEK 1988.

[11] R.Eichler et al., Motivation and Design Study for a B-Meson Factory with High Luminosity, SIN preprint PR-86-13;
K.Wille, Feasibility Study for a B Meson Factory, PSI preprint PR-88-01.

[12] Paul Scherrer Institute (formerly SIN), Proposal for an Electron Positron Collider for Heavy Flavour Particle Physics and Synchrotron Radiation, PSI preprint PR-88-09

[13] U.Amaldi and G.Coignet, Conceptual design of a multipurpose beauty factory based on superconducting cavities, Nucl.Instr.Meth. A260 (187) 7;
U.Amaldi, A one Racetrack Superconducting Accelerator Complex for Bottom Quark and Nuclear Physics Studies, Proc. of the Workshop on Heavy Quarks Factory and Nuclear Physics Facility with Superconducting Linacs, Courmyeur, 14-18 Dec. 1987.

[14] D.B.Cline, A Conceptual Design for a High Luminosity Linear Collider $B\overline{B}$ Factory, Proc. of the UCLA Workshop 'Linear Collider $B\overline{B}$ Factory Conceptual Design', Los Angeles, 26-30 Jan. 1987.

[15] M.K.Sullivan, The Luminosity Upgrade of the PEP Ring, Proc. of the UCLA Workshop 'Linear Collider $B\overline{B}$ Factory Conceptual Design', Los Angeles, 26-30 Jan. 1987.

[16] J.Rees, On the Luminosity of Heteroenergetic Colliding Beam Storage Rings, SLAC/AP-67, 1988;
A.A.Garren, APIARY, Asymmetric Particle Accelerator Research Yard, LBL-Report, 1988

[17] H.Nesemann, W.Schidt-Parzefall and F.Willeke, The Use of PETRA as a B-Factory, contributed paper to the EPAC Accelerator Conf., Rome, June 1988.

[18] A.N.Dubrovin et al., Conceptual Design of a Ring Beauty Factory, contributed paper to the EPAC Accelerator Conf., Rome, June 1988.

[19] SLAC Linear Collider Conceptual Design Report, SLAC-Report-229, 1980.

[20] B.Richter, Proc. of the EPAC Accelerator Conf., Rome, 1988.

[21] P.Oddone, Notes on Scaling Relations for Asymmetric Collisions at a modified PEP Storage Ring, Internal Note, TPC-LBL-87-21.

[22] W.Schmidt-Parzefall and H.D.Schulz, communication to the ARGUS Collaboration.

[23] M.Sands, The Physics of Electron Storage Rings, SLAC-121, 1970.

[24] A.Piwinski, Proc.of the 1977 Particle Accelerator Conf, Chicago, 1977.

[25] K.Wille, B-Factories, Proc. of the EPAC Accelerator Conf., Rome, 1988.

[26] P.Grosse-Wiesmann, Colliding a Linear Electron Beam with a Storage Ring Beam, SLAC-PUB-4545, 1988

[27] R.L.Gluckstern, Nucl.Instr. and Meth. 24 (1963) 381;
A.Wagner, Physica Scripta 23 (1981) 446.

[28] R.Baldini, communication to the PSI/SIN B-factory working group, March 1988.

[29] T.Nakada, private communication.

[30] G.Gratta, A.S.Schwarz and C.Zaccardelli, Vertex Detectors at e^+e^- B Meson Factories, SCIPP-88/04, 1988.

[31] P.Oddone, Detector Considerations, Proc. of the UCLA Workshop 'Linear Collider $B\overline{B}$ Factory Conceptual Design', Los Angeles, 26-30 Jan. 1987.

[32] P.Weilhammer, these Proceedings.

[33] U.Buchner et al., DESY 88-051, 1988

[34] E.Lorenz, Prospects for an Optimized Detector for Υ Physics, Proc. of the Intern. Symposium on Production and Decay of Heavy Hadrons, Heidelberg May 1986.